Comparison of Ergodic Capacities From Wideband MIMO Antenna Measurements in Reverberation Chamber and Anechoic Chamber

Xiaoming Chen, Per-Simon Kildal, *Fellow, IEEE*, Jan Carlsson, *Member, IEEE*, and Jian Yang, *Senior Member, IEEE*

***Abstract*—It has previously been shown that ergodic multiple-input–multiple-output (MIMO) capacity of a multiport antenna system can be conveniently determined from channel measurements in a reverberation chamber. In this letter, we compare such MIMO capacity results to results based on measurements in an anechoic chamber of the embedded far-field functions and efficiencies at all antenna ports. The comparison is performed over two-octaves bandwidth by using the decade bandwidth eleven antenna, a log-periodic dual-dipole array. The agreement between the reverberation chamber results and the anechoic chamber results is good over the entire frequency band 2–8 GHz.**

***Index Terms*—Anechoic chamber, multiple-input–multiple-output (MIMO) capacity, reverberation chamber.**

I. Introduction

MULTIPORT antenna systems have drawn considerable interest due to increased data transmission rate in multipath environments using multiple-input–multiple-output (MIMO) techniques [1]–[3]. In early MIMO literature, antenna elements in a multiport antenna system were assumed isotropic and lossless. The overall antenna effects were examined via impedance-matrix of the multiport antenna and open-circuit correlation (Z-parameter method) in [4]–[6]; using the complete scattering-parameter channel matrix between the transmitting and receiving sides of the MIMO communication system in [7] and [8]; and using both the numerical ray-based channel model and embedded element patterns in [10] and [11].

It was also shown in [10]–[13] that ergodic MIMO capacity can be readily determined from the channel measured in a reverberation chamber, which intrinsically includes all effects of ohmic losses in the antenna and mutual coupling between its ports. There is an alternative way to compute the MIMO capacity using a numerically generated channel matrix (as in [4]–[7]) together with efficiencies and correlations obtained from anechoic chamber measurements. Therefore, the purpose of this letter is to compare and verify the calculated capacities based on measurements in the two chambers. Measurement of an embedded far-field functions anechoic chamber is quite laborious compared to the fast channel measurement in a reverberation chamber. In addition, the anechoic measurement needs to be accomplished by numerically generated channels. The measurements are done by using a bandwidth eleven antenna, which is a log-periodic dual-dipole array with up to eight ports [14].

The work is of particular interest because both the reverberation chamber and anechoic chamber are being considered for standardization of so-called over-the-air (OTA) measurements for characterization of active wireless MIMO stations.

Manuscript received April 04, 2011; accepted May 02, 2011. Date of publication May 10, 2011; date of current version May 26, 2011. This work was supported in part by the Swedish Governmental Agency for Innovation Systems (VINNOVA) within the VINN Excellence Center Chase and by NordForsk.

X. Chen, P.-S. Kildal, and J. Yang are with the Chalmers University of Technology, Gothenburg 412 96, Sweden (e-mail: xiaoming.chen@chalmers.se).

J. Carlsson is with the Electronics Department, SP Technical Research Institute of Sweden, Boras 501 15, Sweden.

Color versions of one or more of the figures in this letter are available online at http://ieeexplore.ieee.org.

Digital Object Identifier 10.1109/LAWP.2011.2152360

II. MIMO Capacity

We assume that the receiver has perfect channel state information (CSI) and that transmitted power is equally allocated among transmitting antenna elements. The maximum available capacity of the multiport antenna system can then be expressed as [1]

$$C_{N_r\times N_t} = E\left\{\log_2\left[\det\left(\mathbf{I}_{N_t} + \frac{\gamma}{N_t}\mathbf{H}_{N_r\times N_t}\mathbf{H}^H_{N_r\times N_t}\right)\right]\right\} \tag{1}$$

where γ is signal-to-noise ratio (SNR), the superscript H is Hermitian operator, $\mathbf{H}_{N_r\times N_t}$ is the channel matrix, N_t and N_r are the number of transmitting and receiving antennas, respectively, and E is statistical expectation taken over samples of the channel matrix describing the fading. The subscripts in (1) will be dropped hereafter for conciseness. $\mathbf{H}$ is normalized so that its Frobenius norm satisfies $\|\mathbf{H}\|_F^2 = N_tN_r$.

The antenna under test is a compact power-balanced two-port antenna in the receive end of the MIMO systems. Therefore, it is judicious to assume ideal transmitting antennas with unity efficiency and no correlation. The overall antenna effects can be included using the Z-parameter method [4]–[6], but only by assuming lossless multiport antenna in single-mode operation. We instead use the following resulting compact formulation in which the values of correlation and efficiency are explicitly shown:

$$C = E\left\{\log_2\left[\det\left(\mathbf{I} + \frac{\gamma e_{\mathrm{emb}}}{N_t}\mathbf{\Phi}^{mc}_{\mathbf{r}}\mathbf{H}\mathbf{H}^H\right)\right]\right\} \tag{2}$$

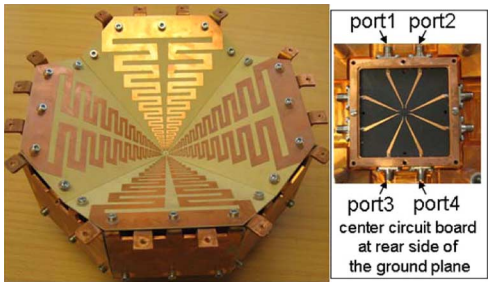

Fig. 1. Photographs of front and back sides of eleven antenna used for validating embedded field function method.

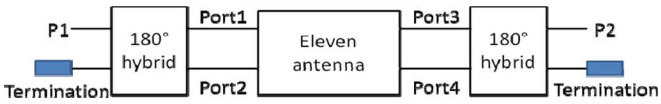

Fig. 2. Diagram of eleven antenna with the four ports of one polarization combined to two ports that are used to produce the results in the present letter.

where e_{emb} is average total embedded radiation efficiency [10] of receive antenna ports, and $\mathbf{\Phi}_{\mathbf{r}}^{mc}$ is the correlation matrix. This takes, for a two-port antenna, the form

$$\mathbf{\Phi}_{\mathbf{r}}^{mc} = \begin{bmatrix} 1 & \rho \\ \rho^* & 1 \end{bmatrix} \tag{3}$$

where ρ is the complex correlation between the two ports. The squared magnitude of the complex correlation is equal to the envelope correlation [15]. Note that (2) is only valid when two antenna ports have approximately the same embedded element efficiencies. The formula can readily be extended for more ports having different efficiencies. For a lossless antenna, both embedded radiation efficiency and correlation can be calculated using S-parameters measured in an anechoic chamber [9], [16], [17]. However, for general lossy multiport antenna, neither the Z-parameter method nor S-parameter method is valid. Then, the complex correlation must be calculated by using [15]

$$\rho = \frac{\iint_{4\pi} G^1_{\mathrm{emb}}(G^2_{\mathrm{emb}})^* d\Omega}{\sqrt{\iint_{4\pi} G^1_{\mathrm{emb}}(G^1_{\mathrm{emb}})^* d\Omega \cdot \iint_{4\pi} G^2_{\mathrm{emb}}(G^2_{\mathrm{emb}})^* d\Omega}} \tag{4}$$

where G^i_{emb} is the complex embedded far-field function of the ith element ($i = 1, 2$), i.e., the far-field function when the other elements are present and terminated with the reference port impedance, normally 50 Ω. Both the embedded radiation efficiencies and the embedded far-field functions can be obtained from anechoic chamber measurements at all ports. This method is called the embedded far-field function method. It can be used both for lossy and lossless antennas.

III. Measurements

The measurements were done using the wideband so-called eleven antenna described in [14] and shown in Fig. 1. In this letter, the four ports for one polarization of the eleven antenna, shown in Fig. 1, are combined to two ports for one polarization, as shown in Fig. 2, by using two wideband 180° hybrids. The result is a two-port antenna with ports P1 and P2 at which capacity is calculated. Each of the ports therefore corresponds to one log-periodic dipole array (one petal), and the log-periodic dipole arrays of the two ports P1 and P2 are parallel. The 180° hybrids have losses between 1.4 dB at 2 GHz and 3 dB at 8 GHz.

A. In Reverberation Chamber

The Bluetest HP reverberation chamber is used for the measurement. It has a size of $1.75 \times 1.25 \times 1.8$ m^3 and is provided with two plate stirrers and platform and polarization stirring [11]. In the measurements, the platform was moved stepwisely to 20 positions spaced by 18°, and for each platform position, each of the two plates moves stepwisely and simultaneously to 10 positions, evenly distributed along the total distance they can move. At each stirrer position and for each of the three wall antennas, the vector network analyzer performed a frequency sweep to sample the channel transfer functions and antenna reflection coefficients as a function of frequency (and stirrer position). Therefore, for each receiving and transmitting antenna element pair, there are 200 samples per frequency point. In order to improve measurement accuracy, 20-MHz frequency stirring (for post-processing) [11] is used. A well-stirred reverberation chamber emulates a rich isotropic multipath environment [11]. It has been shown that ergodic MIMO capacity can be easily determined from reverberation chamber measurement [10]–[13]. First, the average power transfer function is measured using a reference antenna with known total radiation efficiency. The averaging is done over all the stirring samples. The reference level, P_{ref}, is obtained by dividing the average power level with the total radiation efficiency of the reference antenna. The reverberation chamber has three wall antennas, giving the channel matrix $\mathbf{H}_{2\times 3}$ as a function of frequency and stirrer positions, so we chose to evaluate a 2×3 MIMO system from the measured data.

For convenience, we introduce the following notation for the normalized measured channel matrix:

$$\mathbf{H}_{\mathrm{meas}} = \frac{\mathbf{H}_{2\times 3}}{\sqrt{P_{\mathrm{ref}}}}. \tag{5}$$

The MIMO capacity can now be computed from the measured H-matrix by using

$$C = E\left\{\log_2\left[\det\left(\mathbf{I} + \frac{\gamma}{N_t}\mathbf{H}_{\mathrm{meas}}\mathbf{H}_{\mathrm{meas}}^H\right)\right]\right\} \tag{6}$$

where the expectation is taken over all channel samples. Note that the reverberation chamber attenuation and the total radiation efficiency of the wall antennas (transmit side) are calibrated out by (5). Since the three wall antennas in the reverberation chamber are located far away (more than several wavelengths at lowest frequency) from each other on three orthogonal walls, the correlations between them are negligible [11], [15]. Complex correlation in a reverberation chamber can be easily calculated using

$$\rho = \frac{\mathbf{R}(1,2)}{\sqrt{\mathbf{R}(1,1)\mathbf{R}(2,2)}}$$
$$\mathbf{R} = E\{(\mathbf{H}_{\mathrm{meas}} - E[\mathbf{H}_{\mathrm{meas}}])(\mathbf{H}_{\mathrm{meas}} - E[\mathbf{H}_{\mathrm{meas}}])^H\} \tag{7}$$

where $\mathbf{R}$ is covariance matrix.

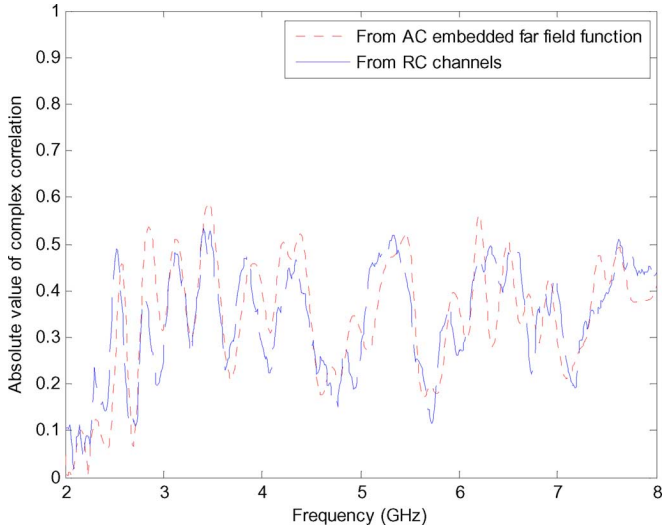

Fig. 3. Comparison of magnitudes of complex correlations calculated from measured embedded far-field functions in the anechoic chamber and MIMO channels in the reverberation chamber.

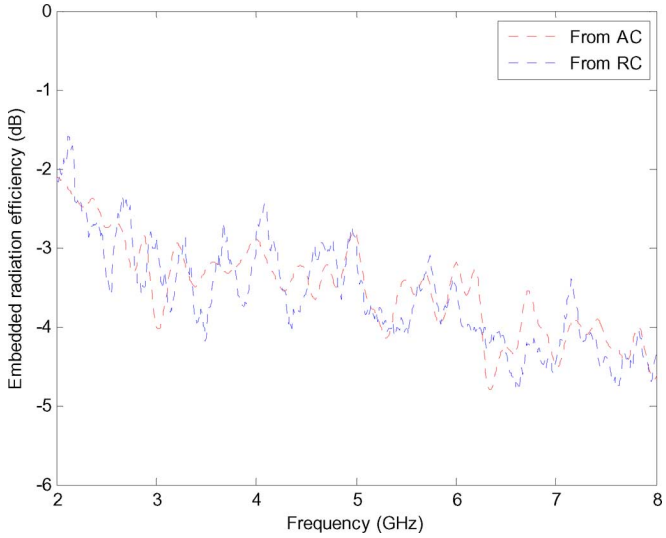

Fig. 4. Comparison of embedded radiation efficiencies measured in anechoic chamber (AC) and reverberation chamber (RC).

B. In Anechoic Chamber

The embedded far-field functions and efficiencies of the eleven antenna were measured in an anechoic chamber (with angular step of 1°) at the Technical University of Denmark (DTU), Lyngby, Denmark. During measurement, the eleven antenna is rotated by an azimuth positioner, and the full-sphere near-field signal is measured on a regular grid by a dual-polarized probe located about 6 m away. The measured signal is then transformed to the far field using the spherical wave expansion and properly correcting for the probe characteristics [18].

C. Results

Fig. 3 compares magnitudes of complex correlations calculated using both embedded far-field functions (4) measured in the anechoic chamber and the correlation obtained from the measured channels in the reverberation chamber (7). As expected, the correlations measured in the anechoic chamber and reverberation chamber agree well with each other. Fig. 4 shows a comparison of embedded radiation efficiencies measured in the anechoic chamber and reverberation chamber. As expected, embedded radiation efficiencies measured in anechoic and reverberation chambers agree well with each other.

Fig. 5 shows the final capacities evaluated from anechoic chamber measurements (embedded far-field functions and efficiencies) and reverberation chamber measurements (MIMO channels) as a function of frequency from 2 to 8 GHz at an SNR of $\gamma = 10$ dB. There is good agreement between embedded far-field function method and reverberation chamber measurement over all frequencies. The slightly decreasing capacity when the frequency increases is due to the fact that the embedded radiation efficiency slightly degrades with increasing frequency.

D. Measurement Uncertainty

In Section II, it was shown that capacity depends on efficiencies and correlations. Thus, the uncertainty of measured capacity depends on the uncertainty of the measured efficiencies and correlations. At high SNR regime, capacity is given by [1]

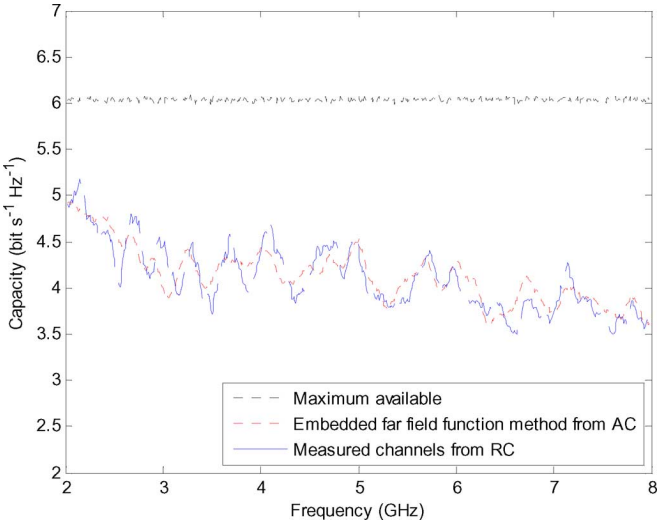

Fig. 5. Comparison of 2×3 MIMO capacities obtained from channel measurements in RC and from embedded far-field functions in AC, all at 10 dB SNR.

$$C = K\log_2\gamma_{\text{eff}} + o(1) \tag{8}$$

where $\gamma_{\text{eff}} = \gamma e_{\text{emb}}$ is effective SNR [13], K denotes the rank of $\mathbf{H}$, and $o(1)$ vanish at high SNR. While correlation (uncertainty) implicitly affects capacity via K, efficiency uncertainty affects capacity explicitly by $\Delta\gamma_{\text{eff}} = \gamma\Delta e_{\text{emb}}$, where Δe_{emb} is the estimated efficiency error. Using Taylor expansion of (8), the estimated capacity error can easily be derived, giving

$$\Delta C = \frac{K}{\gamma_{\text{eff}}\ln 2}\Delta\gamma_{\text{eff}} = \frac{K}{e_{\text{emb}}\ln 2}\Delta e_{\text{emb}}. \tag{9}$$

However, it is well known that correlation smaller than 0.5 (see Fig. 3) has little effect on diversity or MIMO performance [11], [15]. Neglecting correlation uncertainty, the

uncertainty, or standard derivation (STD), of capacity is proportional to the uncertainty (STD) of efficiency.

It would be impractically time-consuming to determine the uncertainty of measured capacity by repeating the measurement procedure many times for measurement in either chamber. Instead, we will determine the uncertainty based on (2) using numerically generated random channels. The STD of efficiencies measured in the Bluetest reverberation chamber is better than 0.5 dB [19], whereas in the anechoic chamber at DTU it is approximately 0.2 dB [18]. For each ergodic capacity simulation, we introduce a random efficiency error with corresponding uncertainty. By repeating this procedure 50 times, we can calculate the STD of the estimated capacity error. It is found that the 0.5-dB efficiency uncertainty of the reverberation chamber gives a capacity STD of 0.12 b/s/Hz, and that the 0.2-dB efficiency uncertainty in the anechoic chamber gives a capacity STD of 0.05 b/s/Hz (at 10 dB SNR). The STD (over frequency) of correlation difference between reverberation and anechoic chamber measurements is 0.08, which means that the correlation STD in either chamber is smaller than 0.08. Using a similar simulation procedure, it is found that correlation uncertainty of 0.08 gives a capacity STD of 0.012 b/s/Hz, which is much smaller than the contribution from the efficiency STD. There are other minor contributions to system error. However, the efficiency uncertainty is found to be the major contribution to capacity uncertainty.

The time used to actually perform the actual measurements covering the whole frequency range was 1.5 h in the reverberation chamber and 10 h in the anechoic chamber. The better accuracy of the anechoic chamber measurement is achieved at the expense of much longer measurement time. Nevertheless, it needs to be mentioned that the capacity uncertainties in the reverberation chamber are small already.

IV. Conclusion

We have compared anechoic chamber and reverberation chamber measurements of ergodic capacity of a MIMO system using an eleven antenna. The far-field functions and efficiencies measured in the anechoic chamber and channel matrices measured in the reverberation chamber give approximately the same results. However, for anechoic chamber measurements, it is necessary to generate the channel matrix numerically and correct it with efficiency and correlation, and the measurement is quite laborious. Note that it is also possible in an anechoic chamber to generate a MIMO fading scenario over the antenna under test. However, this requires a large number of phase- and amplitude-controlled transmitting antennas that considerably increase the price, complexity, and testing times of the system. In contrast, reverberation chambers directly provide the fading channels, including the effects of efficiency, mutual coupling, and correlation. The present study has been done over 2–8 GHz by using the decade bandwidth eleven antenna. Good measurement accuracies are observed in both chambers (anechoic chamber measurement gives better accuracy, but needs more measurement time). The results indicate that this and similar wideband multiport antennas may be conveniently used to compare performances of different types of chambers.

References

[1] C. J. Foschini, "Layered space-time architecture for wireless communication in a fading environment when using multi-element antennas," *Bell Labs Tech. J.*, vol. 1, pp. 41–59, 1996.

[2] A. Paulraj, R. Nabar, and D. Gore, *Introduction to Space-Time Wireless Communication*. Cambridge, U.K.: Cambridge Univ. Press, 2003.

[3] D. Chizhik, F. Farrokhi, J. Ling, and A. Lozano, "Effect of antenna separation on the capacity of BLAST in correlated channels," *IEEE Commun. Lett.*, vol. 4, no. 11, pp. 337–339, Nov. 2000.

[4] R. Janaswamy, "Effect of element mutual coupling on the capacity of fixed length linear arrays," *IEEE Antennas Wireless Propag. Lett.*, vol. 1, pp. 157–160, 2002.

[5] S. Lu, H. T. Hui, and M. Bialkowski, "Optimizing MIMO channel capacities under the influence of antenna mutual coupling," *IEEE Antennas Wireless Propag. Lett.*, vol. 7, pp. 287–290, 2008.

[6] Y. Fei, Y. Fan, B. K. Lau, and J. S. Thompson, "Optimal single-port matching impedance for capacity maximization in compact MIMO arrays," *IEEE Trans. Antennas Propag.*, vol. 56, no. 11, pp. 3566–3575, Nov. 2008.

[7] J. W. Wallance and M. A. Jensen, "Mutual coupling in MIMO wireless systems: A rigorous network theory analysis," *IEEE Trans. Wireless Commun.*, vol. 3, no. 4, pp. 1317–1325, Jul. 2004.

[8] C. Waldschmidt, S. Schulteis, and W. Wiesbeck, "Complete RF system model for analysis of compact MIMO arrays," *IEEE Trans. Veh. Technol.*, vol. 53, no. 3, pp. 579–586, May 2004.

[9] X. Chen, P.-S. Kildal, and J. Carlsson, "Simple calculation of ergodic capacity of lossless two-port antenna system using only S-parameters—Comparison with common Z-parameter approach," presented at the IEEE Int. Symp. Antennas Propag., Spokane, WA, Jul. 3–8, 2011.

[10] K. Rosengren and P.-S. Kildal, "Radiation efficiency, correlation, diversity gain and capacity of a six monopole antenna array for a MIMO System: Theory, simulation and measurement in reverberation chamber," *Proc. Inst. Elect. Eng., Microw., Opt. Antennas*, vol. 152, no. 1, pp. 7–16, Feb. 2005.

[11] P.-S. Kildal and K. Rosengren, "Correlation and capacity of MIMO systems and mutual coupling, radiation efficiency and diversity gain of their antennas: Simulations and measurements in reverberation chamber," *IEEE Commun. Mag.*, vol. 42, no. 12, pp. 102–112, Dec. 2004.

[12] O. Delangre, P. D. Doncker, M. Lienard, and P. Degauque, "Coupled reverberation chamber for emulating MIMO channels," *C. R. Phys.*, vol. 11, pp. 30–36, 2010.

[13] J. F. Valdes, M. A. Fernandez, A. M. Gonzalez, and D. A. Hernandez, "The influence of efficiency on receive diversity and MIMO capacity for Rayleigh-fading channels," *IEEE Trans. Antennas Propag.*, vol. 56, no. 5, pp. 1444–1450, May 2008.

[14] J. Yang, M. Pantaleev, P.-S. Kildal, Y. Karadikar, L. Helldner, B. Klein, N. Wadefalk, and C. Beaudoin, "Cryogenic 2–13 GHz eleven feed for reflector antennas in future wideband radio telescopes," *IEEE Trans. Antennas Propag.*, 2011, to be published.

[15] R. G. Vaughan and J. B. Andersen, "Antenna diversity in mobile communications," *IEEE Trans. Veh. Technol.*, vol. VT-36, no. 4, pp. 149–172, Nov. 1987.

[16] M. V. Ivashina, M. N. M. Kehn, P.-S. Kildal, and R. Maaskant, "Decoupling efficiency of a wideband Vivaldi focal plane array feeding a reflector antenna," *IEEE Trans. Antennas Propag.*, vol. 57, no. 2, pp. 373–382, Feb. 2009.

[17] S. Blanch, J. Romeu, and I. Corbella, "Exact representation of antenna system diversity performance from input parameter description," *Electron. Lett.*, vol. 39, no. 9, pp. 705–707, May 2003.

[18] S. Pivnenko, Private communications, Technical University of Denmark, Lyngby, Denmark, Mar. 2011.

[19] P.-S. Kildal and C. Carlsson, "TCP of 20 mobile phones measured in reverberation chamber," 2002 [Online]. Available: http://www.bluetest.se/downloads/TCPreport-Bluetest-020204.pdf